The effect of stride length on lower extremity joint kinetics at various gait speeds

Robert L. McGrath[1], Melissa L. Ziegler[2], Margaret Pires-Fernandes[3], Brian A. Knarr[4], Jill S. Higginson[5], Fabrizio Sergi[1,5,*]

1 Department of Biomedical Engineering, University of Delaware, Newark, DE 19713, USA

2 Biostatistics Core, College of Health Sciences, University of Delaware, Newark, DE 19713, USA

3 Department of Biomedical Engineering, University of Florida, Gainesville, FL 32611, USA

4 Department of Biomechanics, University of Nebraska, Omaha, NE 68182, USA

5 Department of Mechanical Engineering, University of Delaware, Newark, DE 19713, USA

Abstract

Robot-assisted training is a promising tool under development for rehabilitation of walking function following neurological injury. The challenges in developing the controllers for gait rehabilitation devices that promote desired changes in gait is complicated by the limited understanding of the human response to robotic input. A possible method of controller formulation can be based on the principle of bio-inspiration, where a robot is controlled to apply the change in joint moment applied by human subjects when they achieve a gait feature of interest. However, it is currently unclear how lower extremity joint moments are modulated by even basic gait spatio-temporal parameters.

In this study, we investigated how sagittal plane joint moments are affected by a factorial modulation of two important gait parameters: gait speed and stride length.

We present the findings obtained from 20 healthy control subjects walking at various treadmill-imposed speeds and instructed to modulate stride length utilizing real-time visual feedback. Implementing a continuum analysis of inverse-dynamics derived joint moment profiles, we extracted the global effects of gait speed and stride length on joint moment throughout the gait cycle. Moreover, we utilized a torque pulse approximation analysis to determine the timing and amplitude of torque pulses that approximate the difference in joint moment profiles between stride length conditions, at all gait speed conditions.

Our results show that gait speed has a significant effect on the moment profiles in all joints considered, while stride length has more localized effects, with the main effect observed on the knee moment during stance, and smaller effects observed for the hip joint moment during swing and ankle moment during the loading response. Moreover, our study demonstrated that trailing limb angle, a parameter of interest in programs targeting propulsion at push-off, was significantly correlated with stride length. As such, our study has generated candidate assistance strategies based on pulses of torque suitable for implementation via a wearable exoskeleton with the objective of modulating stride length, and other correlated variables such as trailing limb angle.

Introduction

Stroke is the leading cause of disability in the industrialized world [1]. Following a stroke, survivors often experience hemiparesis; characterized as diminished strength and inability to normally contract muscles on the side of the body contralateral to the lesioned hemisphere [2]. This leads approximately 30% of chronic stroke survivors to experience impaired gait and require walking assistance [3]. As such, restoration of ambulation capacity is a top priority for individuals recovering from a stroke [4].

Standard of care ambulation therapy approaches include treadmill and overground training with and without body weight support. These are highly repetitive movement exercises requiring observation and cues from a physical therapist [5,6]. In recent years, more technologically advanced gait retraining tools have been devised. These include electromechanically-assisting gait retrainers which offer the benefit of reduced physical demand on the physical therapists [5]. Also, functional electrical stimulation (FES)

protocols have been utilized to supplement survivors' diminished capacity to contract [43] muscles during walking [7]. The primary goal of these treatments and indicator of gait [44] performance improvement is gait speed (GS), which is associated with a better quality [45] of life [8,9]. A secondary goal and indicator of function is ambulation endurance, as [46] often measured by the 6-minute walking test, which is significantly associated with [47] scores of community integration [10]. [48]

Currently, it is not well understood how the modulation of assistance provided by a [49] robot or FES unit during gait retraining will lead to improvements in clinical outcome [50] measures. Anterior-posterior ground reaction force, the propulsive force of the foot [51] against the ground during gait, and propulsive impulse, the propulsive force integrated [52] over time, are measures of interest in stroke [11–13]. Previous work has shown that [53] propulsive impulse is positively correlated with GS and negatively correlated with the [54] severity of hemiparesis [11]. Further investigation revealed that posture of the trailing [55] limb at push-off is positively correlated with propulsive impulse in paretic, non-paretic, [56] and healthy control limbs [14]. The posture of the trailing limb at push-off is quantified [57] by one kinematic parameter, known as trailing limb angle (TLA), defined as the angle [58] of the line connecting the hip joint center and foot center of pressure at the instant of [59] peak propulsive force, relative to the global vertical axis [13]. One study examined the [60] relationship between long distance walking function, TLA, and propulsive force in a [61] cohort of chronic stroke patients following twelve weeks of gait retraining. Subjects in [62] this study who experienced improvements in TLA and in propulsive force experienced [63] gains in long distance walking function as measured by the 6-minute walking test [12]. [64] In healthy control subjects, it was observed that when increasing GS, the increase in [65] TLA contributes twice as much as the increase in ankle moment to the resulting [66] increase in propulsive force [15]. Recently, it was observed that in GS modulation by [67] stroke patients, TLA and ankle moment contribute in a 4:1 ratio to propulsive force in [68] the paretic leg and in a 3:1 ratio in the non-paretic leg [13]. Therefore, TLA has been [69] advanced as a variable of interest for improving walking function in stroke patients. [70] However, it is unclear if a gait retraining therapy that targets modulations of TLA will [71] lead to increases in clinical outcome measures. [72]

Our research group is exploring the use of robotic-assisted gait retraining to directly [73] target and modulate TLA. A possible controller could be composed of torque pulses [74]

applied at specific instants during the gait cycle, with the advantage of not constraining [75] gait to follow prescribed trajectories [16]. This approach has been shown in previous [76] studies to be a successful method of robot-assisted gait training [17,18]. However, in [77] absence of models of the human response to a robotic input, it would be difficult to [78] define parameters for such a controller acting on multiple degrees of freedom. A possible [79] method of controller formulation can derive from the principle of bio-inspiration, where [80] a robot is controlled to apply the difference in joint moment applied by human subjects [81] when they achieve a desired gait feature (in this case modulation of TLA), relative to [82] their normal walking condition. Once the effects of the variable of interest have been [83] identified, a rehabilitation robot could be controlled in either assistive, resistive, or [84] perturbation mode to deliver different forms of robot-assisted training [19]. To support [85] the development of such a controller, we first required knowledge about the joint [86] moments applied by healthy control subjects to modulate TLA at a range of GSs. Since [87] TLA has not been a primary measure of interest in the biomechanics literature, we [88] extended our search to a more common variable, likely correlated to TLA, such as stride [89] length (SL). [90]

The joint kinetics associated with GS modulation in healthy control subjects have [91] been thoroughly elucidated in the literature, where an increase in GS is generally [92] associated with increase in magnitude of peak joint moments. A very early investigation [93] examining knee kinetics found increasing GS to be strongly correlated with an increase [94] in peak knee extension moment [20]. Further work found peak hip flexion and extension [95] moments, knee flexion and extensions moments, and ankle plantar and dorsiflexion [96] moments to all increase with GS. However, these changes in joint kinetics to increasing [97] speed were primarily observed at the hip, particularly in extension, and secondarily at [98] the ankle for purposes of support [21]. Most recently, an increase in GS was observed to [99] be associated with an increase in peak hip extension moment during loading response, [100] knee flexion moment in late stance and peak ankle plantarflexion moment [22]. [101]

However, fewer investigations have focused on the joint kinetics associated with the [102] modulation of spatiotemporal parameters such as SL or TLA. Summed joint work has [103] been observed to be strongly correlated with SL in both young and old adults, where [104] young adults primarily utilized swing phase hip work to modulate SL and old adults [105] utilized ankle and knee joint work [23]. An early investigation found stance phase peak [106]

knee extension moment to be strongly correlated with increasing SL [20]. A more recent 107 and in-depth investigation found that as SL increased, peak ankle plantarflexion 108 moment, plantarflexion moment at 40% of stance, and peak knee extension moment all 109 increased, while peak knee flexion moment and peak hip flexion moment decreased [24]. 110

Thus far, the factorial modulation of both GS and SL and resulting hip, knee, and 111 ankle kinetics has not been investigated; as such it is unclear how lower extremity joint 112 moments are modulated by both gait parameters. Addressing this gap of knowledge, we 113 designed an experimental study to establish the effects of GS and SL on the resulting 114 hip, knee, and ankle joint moments. The findings are intended to inform the design of a 115 robotic assistance controller that delivers pulses of torque to the lower extremity joints 116 with optimal timing and amplitude to induce desirable modulations of gait 117 spatiotemporal parameters. 118

Materials and methods 119

Subjects 120

20 healthy adults (10 males, 10 females) were recruited to participate in this study 121 (protocol approved by the University of Delaware Institutional Review Board, protocol 122 no. 619724). Subjects — age (mean $\pm$ std) 21.55 ± 2.50 yrs, height 1.73 ± 0.08 m, body 123 mass 69.20 ± 8.73 kg — were naive to the purpose of the study, and free of orthopedic 124 or neurological disorders affecting walking function. Subjects were required to wear their 125 own comfortable athletic shoes and lightweight clothing for the walking experiment. 126

Setup 127

Subjects walked on an instrumented dual-belt treadmill (Bertec Corp., Columbus OH, 128 USA), as shown in Fig. 1,while wearing thirty-six reflective spherical markers (4 on the 129 pelvis, 4 per thigh, 4 per shank, 2 per knee, and 6 on ankle/foot). An eight camera 130 Raptor-4 passive motion capture system (Motion Analysis Corp., Santa Rosa CA, USA), 131 for subjects 1-14, and ten camera Vicon T40-S passive motion capture system (Oxford 132 Metrics, Oxford, UK), for subjects 15-20, were used to measure marker position in 133 space. Marker data were acquired at 100 Hz, while the treadmill analog force/torque 134

data were acquired at 2 kHz. A 24-in screen was placed at approximately 1500 mm $\hspace{1cm}$ 135

anteriorly from the center of the treadmill, and was used in biofeedback conditions. The $\hspace{1cm}$ 136

screen provided visual feedback about the SL measured at the previous gait cycle $\hspace{1cm}$ 137

(starting and ending at right heel strike) which was updated within 20 ms after each $\hspace{1cm}$ 138

right heel strike. In this experiment, SL for cycle k was defined based on the right heel $\hspace{1cm}$ 139

strike time t and anteroposterior coordinate in the laboratory frame x and constant $\hspace{1cm}$ 140

velocity of the treadmill v: $\hspace{1cm}$ 141

$$\text{SL}_{(k)} = x_{(k+1)} - x_{(k)} + v\left(t_{(k+1)} - t_{(k)}\right) \tag{1}$$

Visual feedback of $\text{SL}_{(k)}$ was provided in terms of the height of a bar, while the $\hspace{1cm}$ 142

desired SL was displayed as a horizontal line with dashed lines indicating the $\pm 10\%$ $\hspace{1cm}$ 143

range. The bar indicating $\text{SL}_{(k)}$ was color coded to indicate whether the measured value $\hspace{1cm}$ 144

was within $\pm 10\%$ of the desired value. During biofeedback sessions, subjects were $\hspace{1cm}$ 145

instructed to modify the length of their strides to achieve the target range, while $\hspace{1cm}$ 146

walking at treadmill-imposed speeds. $\hspace{1cm}$ 147

Procedures $\hspace{1cm}$ 148

Subjects were exposed to a total of fifteen experimental conditions, determined as the $\hspace{1cm}$ 149

combinations of two factors: *i)* GS, with five levels, and *ii)* SL, with three levels. Factor $\hspace{1cm}$ 150

levels were defined in terms of percent change relative to subject self-selected (ss) values $\hspace{1cm}$ 151

to accommodate inter-subject variability in gait parameters. Moreover, to account for $\hspace{1cm}$ 152

the correlation between GS and SL [25], we first measured self-selected stride length $\hspace{1cm}$ 153

(ss-SL) at all speeds, and defined biofeedback-modulated SL conditions as percent $\hspace{1cm}$ 154

changes of SL relative to the ss-SL at any given speed. This experimental setup allowed $\hspace{1cm}$ 155

us to investigate joint kinetics underscoring an increase or decrease of SL relative to the $\hspace{1cm}$ 156

subject's self-selected stride length, at all speeds. $\hspace{1cm}$ 157

Self-selected gait speed $\hspace{1cm}$ 158

A preliminary set of trials were conducted to calculate the subject's self-selected gait $\hspace{1cm}$ 159

speed (ss-GS). Subjects were asked to walk on the treadmill moving at an initial speed $\hspace{1cm}$ 160

of 0.5 m/s, with the treadmill speed gradually increased by intervals of 0.03 m/s, and to $\hspace{1cm}$ 161

indicate when ss-GS was reached. The same procedure was repeated by starting with   162
the treadmill at 1.8 m/s, and decreasing treadmill speed in increments of 0.03 m/s, until   163
the subject indicated that ss-GS had been reached. This procedure was repeated three   164
times and the ss-GS was calculated as the average between the six measured treadmill   165
speed values.   166

Fig 1. The experimental setup - subject walking on instrumented treadmill while
wearing retroflective markers captured by infrared camera system. Real-time visual
feedback provided on screen cues imposed stride length condition.

Non-biofeedback conditions   167

After determination of ss-GS, five walking trials were conducted consisting of ninety   168
seconds of acquired data in the absence of biofeedback. In each trial, treadmill speed   169
was imposed at one of five percentages of the subject's ss-GS [80%, 90%, 100%, 110%,   170
120%] in a randomized order. For each GS, ss-SL was calculated as the mean SL   171
measured at that treadmill speed and utilized for the definition of subsequent desired   172
SL values at each GS.   173

Biofeedback conditions   174

After determination of ss-SL for all five GS conditions, ten additional walking trials   175
were conducted consisting of ninety seconds of data acquisition, two for each treadmill   176
speed value, using biofeedback to cue a desired SL. For each GS, the desired SL was set   177
to be either 17% greater or 17% smaller than the ss-SL at that GS, in a random order.   178
The range of change in SL values was specified based on previous studies showing   179
feasibility of achieving distinguishable gait kinetics when SL was modulated by 17% of   180
the ss value [25]. The investigator initiated data acquisition for each condition when the   181
subject sufficiently achieved the cued SL condition specified via biofeedback.   182

Data analysis   183

Pre-processing   184

Raw marker trajectories were labeled offline. Marker position and force/torque data   185
were fed into a standard Visual3D pre-processing pipeline, which included *i)* noise gating   186

of measured force with a 25 N threshold *ii)* low-pass filtering of marker and force/torque   187

data (Butterworth filter at 6 Hz and 30 Hz cut-off frequency, respectively), *iii)*   188

interpolation of missing marker data with a third order polynomial fit for a maximum   189

gap size of five samples, *iv)* application of the subject-specific model for calculation of   190

joint angles and moments based on inverse kinematics and inverse dynamics algorithms.   191

In a custom MATLAB (MathWorks, Natick, MA, USA) script, hip, knee, and ankle   192

joint angles and moments for the right leg in the sagittal plane were extracted and   193

filtered with a 2nd order low-pass zero-shift Butterworth filter with a cut-off frequency   194

of 15 Hz. Gait cycles were segmented between subsequent heel strike events, defined as   195

the instants at which the vertical ground reaction force changed in value from zero to   196

positive, and remained positive for a minimum of 400ms. Due to events such as marker   197

occlusion or subjects' foot stepping on contralateral force plates, acquired data were   198

manually screened and some gait cycles were excluded from the analysis. A minimum of   199

25 segmented gait cycles were linearly resampled in the [0,100] % gait cycle domain $\tilde{t}$ 200

and averaged at each point in gait cycle to yield an average hip, knee, and ankle joint   201

moment profile $\tau(\tilde{t})$ for each of the 15 experimental conditions for each of the 20   202

subjects.   203

Prior to obtaining average group moment profiles, joint moment profiles were   204

non-dimensionalized. In agreement with [26], the non-dimensional joint moment $\tilde{\tau}$ was   205

calculated for each joint as $\tilde{\tau}(\tilde{t}) = \frac{\tau(\tilde{t})}{W L_l}$, where W is body weight in N, and L_l is leg   206

length in m, measured as the distance between the hip joint center and the floor during   207

straight-leg standing.   208

Protocol validation   209

A non-dimensional GS was defined as the Froude number $Fr = \mathrm{GS}/\sqrt{L_l g}$, where g is   210

the acceleration of gravity. Although several other factors such as body mass and   211

athletic fitness condition account for the variability in ss-GS across individuals [27], the   212

Froude number has been extensively used to describe the conditions underlying the   213

transition from walking to running in several species [28]. As such, we used the Froude   214

number as an index of across-subject dynamic similarity in ss-GS: a smaller variance of   215

Froude numbers within a group of individuals should reflect consistent gait kinetics. We   216

calculated the coefficient of variation $CV_{Fr} = \frac{\sigma_{Fr}}{\mu_{Fr}}$ as the ratio between the standard   217

deviation and the mean of Froude numbers corresponding to the ss-GS condition, and compared it to alternative indices, $CV_{ss-GS} = \frac{\sigma_{ss-GS}}{\mu_{ss-GS}}$ that uses ss-GS, and $CV_{ss-GS_0} = \frac{\sigma_{ss-GS_0}}{\mu_{ss-GS_0}}$ that uses ss-GS normalized by leg length.

Two gait parameters were also calculated; SL was measured using eq. (1), while TLA was calculated as the angle relative to the vertical axis of the line connecting the hip joint center and the position of the center of pressure at the instant of maximum anterior ground reaction force [29]. We conducted a linear correlation between normalized SL ($SL_0 = SL/L_l$) and TLA to validate our protocol as suitable to inform the design of TLA-oriented robot-aided training protocols

Continuum analysis

We sought to determine if the two factors GS and SL had any significant effect on the sagittal plane moment profiles for the hip, knee, and ankle joint $\bar{\tau}(\tilde{t})$, and, if so, at which phase of a gait cycle was a significant effect of either factor measured. We conducted an analysis for the main effects of the two factors, GS and SL, by implementing a repeated-measure 2-way ANOVA on the mean joint moment profiles measured from each subject and experimental conditions, spanning exhaustively the 15 combinations of factors. ANOVA was conducted to test the null hypothesis that neither factor (GS and SL), nor their interaction, induce a significant effect on joint moment at any time point.

Since the dependent variable $\bar{\tau}(\tilde{t})$ is one-dimensional (1D) smoothed time series including highly temporally correlated data, and not a zero-dimensional scalar quantity (e.g. peak torque, range of motion, etc.), definition of confidence intervals and control of false positive rates (FPR) requires proper correction for multiple comparisons that accounts for the temporal correlations in the input time series [30]. We used the software SPM1D, a parametric statistical testing method developed for nD time series [31], to control for FPR in the analysis of normalized joint moment profiles $\tilde{\tau}(\tilde{t})$, and quantify the effect of both factors (GS and SL) and of their interaction on the dependent variable in different phases of the gait cycle. 2-way repeated-measure ANOVA was conducted using the SPM1D software package, using SPM1D's function `anova2rm` [31]. Inference was conducted setting a corrected type-I error rate $\alpha = 0.05$ based on SPM1D's correction based on random field theory (RFT) to estimate the smoothness in the input data.

After the main effect analysis, we conducted pairwise comparisons to establish the specific effect of SL on the measured joint moment profiles, testing for the null hypothesis that the mean profiles measured at the same speed for nominal and bio-feedback modulated SL conditions were not different from one another at any time point. This resulted in two comparisons (ss vs. increased SL, and ss vs. decreased SL) per speed, per joint, for a total of $n_{comp} = 30$ pairwise comparisons. Pairwise comparisons were conducted using two-tailed paired t-tests using SPM1D function `ttest_paired`, and defining thresholds t-scores for significance at $\alpha = 0.05$ using a Bonferroni correction ($n = n_{comp}$) on the paired difference thresholds calculated by SPM1D.

Torque pulse approximation

We then conducted a second analysis with the specific purpose of deriving candidate primitives for a controller based on the application of pulses of torque as select phases of the gait cycle. As such, we sought to approximate the effect of SL modulation on joint moment profiles with a series of rectangular pulses of torque. First, the normalized difference $\Delta\bar{\tau}(\tilde{t})$ of subject specific average joint moment profiles $\tau(\tilde{t})$ between conditions of positive or negative SL, and ss SL, at each gait speed j were extracted as:

$$\Delta\bar{\tau}_{\pm}^{(j)}(\tilde{t}) = \frac{\tau_{\pm\text{SL}}^{(j)}(\tilde{t}) - \tau_{\text{ss-SL}}^{(j)}(\tilde{t})}{\text{Max}\left(\tau_{\text{ss-SL}}^{(j)}(\tilde{t})\right) - \text{Min}\left(\tau_{\text{ss-SL}}^{(j)}(\tilde{t})\right)} \tag{2}$$

The rectangular torque pulses $P_{\pm}(\tilde{t})$ were defined using a constant duration of 10% of gait cycle, variable time of application α_l, and amplitude A_l as in the equation:

$$P_{\pm}(\tilde{t}) = \sum_{l=1}^{N} A_{l,\pm}\text{rect}\left(\frac{\tilde{t} - \alpha_{l,\pm}}{10}\right) \tag{3}$$

For this specific work, we examined the one and two pulse ($N = 1, 2$) approximation of the function $\Delta\bar{\tau}_{\pm}^{(j)}(\tilde{t})$, and used nonlinear constrained optimization—MATLAB function's `fmincon`—to find the values of parameters A and α that minimize the norm of residuals $P_{\pm}(\tilde{t}) - \Delta\bar{\tau}_{\pm}^{(j)}(\tilde{t})$. In this optimization, the domain for α_l was defined as the set of integers between 5% and 95%, providing a quantization in the time of application of torque pulses equal to 1% of a gait cycle duration. For each joint, we divided the

estimated pulses into two different groups depending on whether their amplitude was in the positive, or negative direction (i.e., positive extension for the hip and knee joint, positive plantarflexion for the ankle joint).

With the purpose of identifying location and amplitude of application of pulses of torque that would approximate the SL-specific difference between joint moment profiles measured at all speeds, we performed statistical analyses to determine if any of the outcome measures, pulse magnitude and location, were significantly modulated by any of the three independent variables (i.e., joint, direction of SL modulation, and sign of applied pulse). For the purposes of our analysis, pulse magnitude is the absolute value of pulse amplitude. Four separate linear mixed effects models (SAS V9.4, SAS Institute, Cary, NC) were performed on the one and two pulse approximations for both the pulse magnitude and location data sets to test the null hypothesis that no independent variable had an effect on the outcome measures. The models included fixed effects for each of the independent variables as well as all two-way and one three-way interaction between them. Heterogeneity due to trials completed under different gait speed conditions, and multiple pulses in the case of the two pulse approximation were accounted for by the inclusion of random effects. Correlation between multiple measurements taken on the same subject were accounted for by the inclusion of a repeated measure effect. Upon comparing nested model Akaike information criterion (AIC) values; the lowest AIC value came from the unstructured covariance structure and was therefore selected for the final models. In case of effects statistically significant at the $\alpha < 0.05$ level, effects and interactions were further investigated through post hoc Tukey-Kramer tests ($\alpha = 0.05$).

Results

Protocol validation

The mean Froude numbers with 95% confidence intervals, across gait speed conditions, are shown in the left of Fig. 2. The use of the Froude did not reduce the across-subject variability in ss-GS, with $CV_{Fr} = 0.106$, slightly greater than $CV_{\text{ss-GS}} = 0.104$, and both smaller than $CV_{\text{ss-GS}_0} = 0.121$. All differences account for an effect size that can

be considered very small. To determine if the imposed biofeedback effectively   303
modulated SL in healthy subjects, we assessed the distribution of SL values across all   304
three feedback conditions at the five different gait speeds, shown in the center of Fig. 2.   305
The change in mean SL from ss-SL across all ten feedback conditions for all subjects   306
was equal to $\pm14.94\%$, close to the target $\pm17\%$ value. The maximum standard   307
deviation of SL_0 values for all five non-feedback conditions, averaged across all subjects, 308
was relatively small ($\sigma_{\max} = 3.86\%$). Based on these measures, we conclude that the 309
protocol significantly modulated values of SL and GS, such that statistical analysis may   310
be performed.   311

Fig 2. (Left) the distribution of mean Froude numbers with 95% confidence intervals at the various treadmill imposed GSs, (center) normalized stride lengths measured at various speeds and biofeedback conditions. The box plot shows the median as a horizontal line, and the box at 25% and 75% percentiles, with whiskers extending to $\pm 3\sigma$, and (right) mean trailing limb angle and mean normalized stride length for each of the 15 conditions for each of the 20 subjects. Linear regression indicates that there is a strong correlation (r = 0.87) between the two measures.

We calculated the mean TLA and SL_0 value for each of the 15 conditions for all   312
subjects to assess the correlation between these measures; see right side of Fig. 2.   313
Linear regression demonstrated a strong correlation (r = 0.87) between SL_0 and TLA,   314
which indicates that subjects also modulated TLA while achieving biofeedback cued SL   315
modulation. The group analysis of joint moments in the three SL conditions across five   316
GS conditions is depicted in Fig. 3   317

Fig 3. Effect of gait speed (GS) and stride length (SL) modulation on the normalized joint moments $\bar{\tau}$. Joints are organized by row, GS are organized by columns, relative to the subject-specific ss-GS. Conditions corresponding to cued SL values are superimposed on each plot. Lines indicate the group mean, with the shaded region indicating the standard error.

Continuum analysis   318

The continuum analysis showed an effect of GS on the normalized joint moment profiles,   319
where a significant effect of GS was detected for a total 82.2%, 78.8% and 64.1% of the   320
gait cycle for the hip, knee, and ankle joint respectively, as shown in Fig. 4. The effect 321
of SL on hip joint moment was significant for four short clusters in early to midstance,   322
at push-off, and two clusters spanning the majority of swing for a total duration of a   323

significant effect of SL on hip joint moment of 61.4% of the gait cycle. A stronger effect, both in magnitude and duration, was measured at the knee joint with the first two clusters spanning early stance. The effect of SL on knee joint moment was highly significant from midstance until the end of gait cycle; for a total of 87.7% of the gait cycle with a significant effect. A strong effect of SL was detected at the ankle joint for 6 clusters; at weight acceptance, push-off and four clusters covering approximately half of swing for a total of 39.3% of the gait cycle. The interaction between the two factors was significant for the hip for four clusters; mainly during the transition from stance to swing and during late swing for a total of 27.1% of the gait cycle. For the knee, the interaction was significant for 5 clusters; 2 short intervals during early stance, late stance, early swing, and midswing for a total of 33.2% of gait cycle. For the ankle, the interaction was only significant for two clusters, late stance and mid swing for a total of 18.1% of gait cycle. Pairwise comparisons of joint moment profiles measured at nominal and biofeedback-modulated SL values are shown in Fig. 5 – 7 for all GSs.

Fig 4. Main effects of gait speed (GS) and stride length (SL), and of their interaction, on the normalized joint moment profiles during normal walking, as described by the 1D time series of F-scores extracted by the 2-way repeated measure ANOVA. The threshold F score for each experimental condition is reported by the red dashed line, and values above (shaded in green) correspond to a significant group effect of the factor, at the corresponding gait cycle instant, for a corrected type I error rate $\alpha < 0.05$.

Pairwise comparisons for the hip joint show that during increased SL conditions (Fig. 5, right), hip flexion moment during early swing and hip extension moment during late swing decreased. The first comparison reached significance in three out of five GS conditions, while the second effect was significant at all GS values. No effect of SL on hip joint moment during stance were observed in more than one GS condition. A similar pattern is observed when SL is decreased via biofeedback (Fig. 5, left).

Fig 5. T-scores resulting from pairwise comparisons of normalized hip torque moment at normal and modulated SL (columns), measured at the same GS, for each GS (row). Red dashed lines show the threshold t value that provides a corrected type I errfor rate $\alpha = 0.05$, extracted using a Bonferroni correction that accounts for all pairwise comparisons $n_{comp} = 30$.

For the knee, during increased SL conditions (Fig. 6, right), knee extension moment increased in early stance, while knee flexion moment increased in late stance. During the swing phase, knee extension moment decreased in early swing, and knee flexion

moment decreased in late swing. The effects reported were significant at the group level 347

at all GSs. A similar pattern was observed for a decrease of SL, with smaller effects for 348

the increased knee extension at early stance (a significant effect was measured only in 349

four out of five GS conditions, Fig. 6, right). 350

Fig 6. T-scores resulting from pairwise comparisons of normalized knee torque moment at normal and modulated SL (columns), measured at the same GS, for each GS (row). Red dashed lines show the threshold t value that provides a corrected type I error rate $\alpha = 0.05$, extracted using a Bonferroni correction that accounts for all pairwise comparisons $n_{comp} = 30$.

For the ankle, during increased SL conditions (Fig. 7, right), ankle dorsiflexion 351

moment increased at early stance, while no effect on plantarflexion moment was 352

measured at push-off. A similar pattern was observed for a decrease of SL (Fig. 7, 353

right), with a greater effect measured in terms of increased plantarflexion moment at 354

early swing (significant at all GSs). In two out of five GS conditions, the decreased SL 355

condition exhibited a reduced ankle plantarflexion moment during push-off significant at 356

the group level. 357

Fig 7. T-scores resulting from pairwise comparisons of normalized ankle torque moment at normal and modulated SL (columns), measured at the same GS, for each GS (row). Red dashed lines show the threshold t value that provides a corrected type I error rate $\alpha = 0.05$, extracted using a Bonferroni correction that accounts for all pairwise comparisons $n_{comp} = 30$.

Torque pulse approximation 358

Figures 8 and 9 show the distribution of torque pulse magnitudes grouped by joint for 359

both positive and negative SL modulations for the one and two pulse approximations, 360

respectively. 361

Fig 8. Histogram of one pulse approximation normalized amplitudes, sorted by SL modulation and joint.

Fig 9. Histogram of two pulse approximation normalized amplitudes, sorted by SL modulation and joint.

The results of the linear mixed effects model analyses for torque pulse magnitude are 362

shown in Tables 1 and 2. A significant effect of factors joint and pulse sign, and a 363

significant interaction between factors joint and SL modulation were observed for the 364
one and two pulse approximations. The interaction between factors joint, SL 365
modulation, and pulse sign was significant for the two pulse approximation at the 366
selected significance level. The Tukey-Kramer post hoc test for the joint and SL 367
modulation interaction, shown in Tables 3 and 4, was used to establish the presence of 368
significant differences in pulse magnitude means between joints for SL modulation 369
conditions, separately. The mean and standard deviation of the joint magnitudes are 370
shown in Figures 10 and 11. In the one and two pulse approximations, for both SL 371
modulation conditions, the normalized torque pulse magnitudes of the knee joint were 372
greater than both the hip and ankle joints. The only significant difference between hip 373
and ankle joint magnitudes existed for the positive SL modulation condition for the two 374
pulse approximation. 375

Table 1. Magnitude linear mixed effects model results for the one torque pulse
approximation

Factor	DF	F Value	Prob >F
Joint	2	130.63	**<0.001**
SL Mod	1	0.50	0.482
Pulse Sign	1	5.44	**0.020**
Joint x SL Mod	2	12.41	**<0.001**
Joint x Pulse Sign	2	1.15	0.318
SL Mod x Pulse Sign	1	0.03	0.862
Joint x SL Mod x Pulse Sign	2	2.14	0.120

Table 2. Magnitude linear mixed effects model results for the two torque pulse
approximation

Factor	DF	F Value	Prob >F
Joint	2	154.81	**<0.001**
SL Mod	1	0.21	0.645
Pulse Sign	1	24.68	**<0.001**
Joint x SL Mod	2	10.75	**<0.001**
Joint x Pulse Sign	2	2.91	0.055
SL Mod x Pulse Sign	1	2.05	0.152
Joint x SL Mod x Pulse Sign	2	3.99	**0.019**

Table 3. Magnitude Tukey-Kramer post hoc test results for the one torque pulse
approximation

	Mean (Std Err Dif)		
SL Mod	Hip - Knee	Hip - Ankle	Knee - Ankle
+SL	**-0.172 (0.014)**	0.022 (0.008)	**0.194 (0.014)**
-SL	**-0.094 (0.011)**	0.010 (0.010)	**0.104 (0.012)**

Table 4. Magnitude Tukey-Kramer post hoc test results for the two torque pulse approximation

SL Mod	Mean (Std Err Dif)		
	Hip - Knee	Hip - Ankle	Knee - Ankle
+SL	**-0.115 (0.009)**	**0.019 (0.005)**	**0.135 (0.009)**
-SL	**-0.069 (0.007)**	0.015 (0.006)	**0.085 (0.008)**

Fig 10. Pulse magnitude by joint and SL modulation for the one pulse approximation (mean ± standard deviation). Asterisks indicate pairwise comparisons significant at the $p < 0.05$ corrected level.

Fig 11. Pulse magnitude by joint and SL modulation for the two pulse approximation (mean ± standard deviation). Asterisks indicate pairwise comparisons significant at the $p < 0.05$ corrected level.

Figures 12 and 13 show the distributions of torque pulse location in gait cycle. All pulses were combined across the twenty subjects and five gait speed conditions and grouped by joint and SL modulation condition for the one and two pulse approximations, seperately. For representation purposes, within each histogram, the pulses are divided into positive and negative groups according to the sign of pulse amplitude $\Delta\bar{\tau}_{\pm}^{(j)}(\tilde{t})$, and then further divided into two more categories (i.e. small and large) based on whether their magnitude was smaller or larger than the group median.

Fig 12. Histogram of one pulse approximation locations in gait cycle, sorted by pulse amplitude sign and magnitude.

Fig 13. Histogram of two pulse approximation locations in gait cycle, sorted by pulse amplitude sign and magnitude.

The linear mixed effects model results for torque pulse location in gait cycle are shown in Tables 5 and 6. The analyses yielded a highly significant effect of joint and interactions between joint and pulse sign, SL modulation and pulse sign, and joint, SL modulation, and pulse sign for both pulse approximations. The factor of pulse sign was only significant for the one pulse approximation and the factor of SL modulation and interaction of joint and SL modulation were only significant for the two pulse approximation.

The three-way interaction between joint, SL modulation, and pulse sign was broken down using the Tukey-Kramer post hoc test to find the significant differences between torque pulse location, for a given joint, under different combinations of factors SL

Table 5. Location linear mixed effects model results for the one torque pulse approximation

Factor	DF	F Value	Prob >F
Joint	2	49.32	**<0.001**
SL Mod	1	2.14	0.146
Pulse Sign	1	31.48	**<0.001**
Joint x SL Mod	2	0.53	0.589
Joint x Pulse Sign	2	13.61	**<0.001**
SL Mod x Pulse Sign	1	166.41	**<0.001**
Joint x SL Mod x Pulse Sign	2	78.42	**<0.001**

Table 6. Location linear mixed effects model results for the two torque pulse approximation

Factor	DF	F Value	Prob >F
Joint	2	55.62	**<0.001**
SL Mod	1	8.62	**0.004**
Pulse Sign	1	3.01	0.083
Joint x SL Mod	2	3.30	**0.039**
Joint x Pulse Sign	2	22.11	**<0.001**
SL Mod x Pulse Sign	1	176.74	**<0.001**
Joint x SL Mod x Pulse Sign	2	147.21	**<0.001**

modulation and torque pulse sign. We were especially interested in testing whether   393
there were specific instants of time where the application of a positive torque pulse   394
would modulate SL in a certain direction, and, simultaneously, where the application of   395
a negative torque pulse would modulate SL in the opposite direction. As such, for each   396
joint, we conducted two pairwise comparisons: one to compare the location variables   397
measured for positive pulse torque sign and positive SL modulation with the variables   398
measured for negative pulse torque sign and negative SL modulation, and a second one   399
to compare the location variables measured for positive pulse torque sign and negative   400
SL modulation with the variables measured for negative pulse torque sign and positive   401
SL modulation. All of these pairwise comparisons are reported in Tables 7 and 8. In the   402
one pulse approximation, both pairwise comparisons for the hip and ankle joint yielded   403
a relatively large difference in mean location, with three out of the four comparisons   404
statistically significant. On the contrary, the pairwise comparisons for the knee yielded   405
small (1 - 2% gait cycle duration) and statistically insignificant mean differences. This   406
indicates that for the knee joint, clustering of torque pulses by location was symmetrical   407
in reversed stride length conditions, with negative pulses in negative SL conditions   408
clustering around a similar value as positive pulses in positive SL conditions, and   409
positive pulses in negative SL conditions clustering around a similar value as negative   410

pulses in positive SL conditions, while the same effect was not measured for the hip and ankle joints. However, this pattern was not observed in the two pulse approximation; in which one out of the four hip and ankle joint comparisons and one of the two knee joint comparisons were statistically significant. For the one and two pulse approximations, all knee joint mean comparisons were below 10% gait cycle, the width of the torque pulses used for the approximation.

Table 7. Location Tukey-Kramer post hoc testing for the one torque pulse approximation

Joint	Mean[1] - Mean[2] (Std Err Dif)	
	[1] +SL +Sign [2] -SL - Sign	[1] - SL + Sign [2] +SL -Sign
Hip	-9 (7)	**-19 (5)**
Knee	-1 (2)	-2 (2)
Ankle	**-11 (3)**	**-13 (3)**

Table 8. Location Tukey-Kramer post hoc testing for the two torque pulse approximation

Joint	Mean[1] - Mean[2] (Std Err Dif)	
	[1] +SL +Sign [2] -SL - Sign	[1] - SL + Sign [2] +SL -Sign
Hip	-3 (4)	**-20 (4)**
Knee	**8 (2)**	6 (2)
Ankle	-1 (2)	-3 (2)

Discussion

We exposed subjects to a factorial modulation of gait speed (GS) and stride length (SL) and utilized inverse dynamics to estimate the lower extremity joint moments in the sagittal plane. With our protocol, we modulated SL of individuals significantly between conditions, with a mean change in SL equal to $\pm15\%$ of the self-selected value, close to the target $\pm17\%$ with a relatively low standard deviation of 3.86%. Furthermore, inter-individual variability in self-selected gait speed (ss-GS) was reasonably small, with a coefficient of variation $CV_{\text{ss-GS}} = 0.103$. Based on these measures, it is apparent that our protocol significantly modulated both SL and GS, such that statistical analysis may be performed to assess changes in joint kinetics arising from exposure to these conditions. Our analysis showed a strong correlation (r = 0.87) between SL and TLA, indicating that TLA was indirectly modulated through the explicit cueing of SL modulation. Our

data analyses focused primarily on the effects on joint kinetics introduced by $\quad$ 429

modulation of SL at various GSs and secondarily on the effects introduced by GS. $\quad$ 430

The most prominent effects of SL modulation on joint moment were observed for the $\quad$ 431

knee joint. Simple visual inspection of the normalized joint moment profiles, Fig. 3, $\quad$ 432

clearly indicates the effect of SL on joint moment, where stance phase peak extension $\quad$ 433

moment and peak flexion moment increase with increasing SL as well as increasing GS. $\quad$ 434

Increasing peak knee extension moment with SL was also observed previously [20, 24] $\quad$ 435

while increasing peak flexion moment is in contrast with the previously observed $\quad$ 436

decreasing peak knee flexion moment [24]. This contrasting result could be attributed $\quad$ 437

to important differences with the experimental paradigm pursued in [24], where SL and $\quad$ 438

cadence, and not SL and gait speed, were cued. These observations are validated by the $\quad$ 439

continuum analysis, where a main effect of SL was observed for 87.7% of the gait cycle, $\quad$ 440

the highest percentage of all three joints. The significant effect of SL on peak flexion $\quad$ 441

and extension moments during stance is supported by the pairwise comparisons between $\quad$ 442

joint torque measured at different SL conditions (Fig. 6). Here, significant effects at $\quad$ 443

early stance support an increase in knee extension moment with increasing SL, and $\quad$ 444

significant effects in late stance support an increase in knee flexion moment with $\quad$ 445

increasing SL. These effects introduced by increases in SL are also captured by the $\quad$ 446

torque pulse approximations through visual inspection of the pulse approximation $\quad$ 447

histograms 12 and 13 and the findings of their associated linear mixed effects model $\quad$ 448

pulse location analyses. Our findings indicate that an increase in SL is associated with $\quad$ 449

positive pulses of torque – an increase in extension moment – in early stance, and $\quad$ 450

negative pulses – an increase in flexion moment – in late stance. The reverse pattern is $\quad$ 451

observed for SL decrease in which there are negative pulses of torque – decreasing $\quad$ 452

extension moment – in early stance, and positive pulses of torque – decreasing flexion $\quad$ 453

moment – in late stance. This pattern is supported by the Tukey-Kramer post hoc one $\quad$ 454

pulse approximation results for the joint, SL modulation, and pulse sign interaction $\quad$ 455

effect of the pulse location linear mixed effects model analyses. Furthermore, for the one $\quad$ 456

pulse approximation, there is no significant difference in location between pulses of $\quad$ 457

positive SL and negative sign and pulses of negative SL and positive sign. The lack of $\quad$ 458

significant difference in the location of these specific pulse groups supports the $\quad$ 459

observation of a systematic pulse pattern at the knee which reverses in sign with $\quad$ 460

reversal of SL modulation direction. Another indication of the effect of SL modulation   461
on knee joint moment derives from the fact that the one and two pulse approximations   462
yielded a significant effect of the joint and SL modulation interaction on magnitude   463
($p < 0.001$) with Tukey-Kramer post hoc tests indicating the knee having the greatest   464
normalized pulse magnitude (Tables 3 and 4 and Figures 10 and 11). Overall, our   465
findings indicate that the effects of SL on the knee joint moment can be described as   466
follows: knee extension moment at early stance and knee flexion moment at late stance   467
are increased for an increase in SL, while knee extension moment at early stance and   468
knee flexion moment at late stance are decreased for a decrease in SL.   469

Significant effects of SL modulation were also observed at the hip joint. As indicated   470
by the main effect of SL quantified by the continuum analysis, there are two major   471
intervals of significance: early swing and late swing. These effects in swing are visible   472
upon inspection of the group moment profiles where an increase in SL is associated with   473
a decrease in flexion moment during early swing and a decrease in extension moment   474
during late swing. The statistical significance of these observations is clearly indicated   475
by the pairwise comparisons of SL modulation at different speeds shown in Fig. 5. Here,   476
in all pairwise comparisons, an increase in SL is associated with a significant interval in   477
early swing and in late swing. Another indication on how SL modulates hip moment   478
during the swing phase is provided by the torque pulse approximation histograms,   479
which consistently depict a grouping of negative pulses in late swing for positive change   480
in SL and positive pulses in late swing for negative change in SL. However, the pattern   481
is less clear than the one seen at the knee joint because of the small magnitude of those   482
pulses occurring in the swing phase, which even though they are representative of a   483
statistically significant effect, they account for a small amplitude (see distribution of   484
larger pulses in Fig. 12 and 13). As such, the effect in SL obtained for a change in   485
magnitude of the applied torque is not symmetrical (Tables 7 and 8), as demonstrated   486
by the Tukey-Kramer post hoc tests for both pulse approximations. These groupings of   487
pulses in late swing are likely associated with the decrease in hip extension moment   488
during late swing associated with increasing SL.   489

Relatively small effects of SL modulation were observed at the ankle joint. Most   490
prominently, during loading response, dorsiflexion moment increases with an increase in   491
SL as also can be observed in the group moment profiles. This is supported by the main   492

effect of SL measured via the continuum analysis, where the first 10% of gait cycle shows a significant effect of GS on joint moment. This is further supported by the observation of a significant increase in dorsiflexion moment (negative change) for increases in SL, in nine of the ten pairwise comparisons at all speeds, shown in Fig. 7. Another observed effect through the pairwise comparisons conducted via the continuum analysis is the increase in plantarflexion moment at early swing with increasing SL. This effect can be confirmed through visual inspection of the group moment profiles. In contrast with previous work [24], we did not observe a consistent increase in peak plantarflexion moment with increasing SL, with only the three highest speed conditions showing a significant effect for the transition from -17% ss to ss-SL, and no significant effects measured for an increase in stride length over the self-selected value.

Conclusion

Our study has measured the effects of stride length (SL) on the lower extremity joint moment profiles at different speeds, demonstrating several consistent effects in our population. The main effects of increasing SL at the knee include an increase in knee extension moment at early stance and an increase in flexion moment at late stance. At the hip, the main effects of increasing SL are a decrease in flexion moment during early swing and a decrease in extension moment during late swing. For an increase in SL, the ankle primarily exhibits an increase in dorsiflexion moment during loading response. Given the observed linear relationship between SL_0 and TLA, pulse torque approximation patterns associated with SL modulation are also associated with TLA modulation. These findings suggest that a possible joint moment assistance strategy based on pulses of torque applied primarily at the hip and the knee joint could induce modulations in both SL and TLA. According to our analysis, the application of positive pulses of torque in early stance and a negative pulse in late stance to the knee appear to be suitable candidate assistance strategies to support an increase of SL and TLA during walking. If pulse torque assistance is to be applied at an additional joint, pulse torque assistance could be applied at the hip with a negative pulse applied during late swing.

This study has some limitations. The methods pursued in this paper are based on a group analysis of joint moment profiles measured via inverse-dynamics. As such, it is

possible that the most successful assistance strategies may significantly change between $_{523}$ different individuals. Therefore, the group analysis based assistance strategy candidate $_{524}$ could be best utilized as an initial estimate and assistance strategies could be iteratively $_{525}$ optimized for each subject using human-in-the-loop optimization, like it has been done $_{526}$ for single-joint assistance schemes [17]. $_{527}$

Moreover, the proposed assistance strategy candidate is based on the assumption $_{528}$ that human contribution will not change when an assistive torque is applied via a $_{529}$ wearable exoskeleton, such that the combination of torques applied by the two agents $_{530}$ would result in a simple summation. However, it is well known that the human $_{531}$ neuromuscular system is non-linear [32] and it involves complex feedback loops [33]. As $_{532}$ such, the response to a torque perturbation at a specific instant in gait cycle will be $_{533}$ difficult to predict. Given the difficulty of formulating a model of the human response $_{534}$ to these assistance strategies, once again the results of this analysis work could be used $_{535}$ as an initial estimate to be iteratively optimized for each subject using $_{536}$ human-in-the-loop optimization. $_{537}$

Acknowledgments $_{538}$

References $_{541}$

1. Belda-Lois JM, Mena-del Horno S, Bermejo-Bosch I, Moreno JC, Pons JL, Farina $_{542}$ D, et al. Rehabilitation of gait after stroke: a review towards a top-down $_{543}$ approach. Journal of NeuroEngineering and Rehabilitation. 2011;8(66). $_{544}$ doi:10.1186/1743-0003-8-66. $_{545}$

2. Olney SJ, Richards C. Hemiparetic gait following stroke. Part I: Characteristics. $_{546}$ Gait and Posture. 1996;4:136–148. doi:10.1016/0966-6362(96)01063-6. $_{547}$

3. Go AS, Mozaffarian D, Roger VL, Benjamin EJ, Berry JD, Blaha MJ, et al. $_{548}$ Heart Disease and Stroke Statistics - 2014 Update: A report from the American $_{549}$ Heart Association. vol. 129; 2014. $_{550}$

4. Harris JE, Eng JJ. Goal Priorities Identified through Client-Centred Measurement in Individuals with Chronic Stroke. Physiotherapy Canada. 2004;56(3):171–176. doi:10.1167/iovs.07-1072.Complement-Associated.

5. Mehrholz J, Thomas S, Werner C, Kugler J, Pohl M, Elsner B. Electromechanical-assisted training for walking after stroke (Review). Cochrane Database of Systematic Reviews. 2017;(5). doi:10.1002/14651858.CD006185.pub4.www.cochranelibrary.com.

6. States RA, Pappas E, Salem Y. Overground physical therapy gait training for chronic stroke patients with mobility deficits (Review). Cochrane Database of Systematic Reviews. 2009;(3). doi:10.1002/14651858.CD006075.pub2.www.cochranelibrary.com.

7. Kafri M, Laufer Y. Therapeutic Effects of Functional Electrical Stimulation on Gait in Individuals Post-Stroke. Annals of Biomedical Engineering. 2015;43(2):451–466. doi:10.1007/s10439-014-1148-8.

8. Schmid A, Duncan PW, Studenski S, Lai SM, Richards L, Perera S, et al. Improvements in Speed-Based Gait Classifications Are Meaningful. Stroke. 2007;38:2096–2101. doi:10.1161/STROKEAHA.106.475921.

9. Dickstein R. Rehabilitation of Gait Speed After Stroke: A Critical Review of Intervention Approaches. Neurorehabilitation and Neural Repair. 2008;22(6):649–660. doi:10.1177/1545968308315997.

10. Mayo NE, Wood-Dauphinee S, Ahmed S, Gordon C, Higgins J, McEwen S, et al. Disablement following stroke. Disability and Rehabilitation. 1999;21(5-6):258–268. doi:10.1080/096382899297684.

11. Bowden MG, Balasubramanian CK, Neptune RR, Kautz SA. Anterior-Posterior Ground Reaction Forces as a Measure of Paretic Leg Contribution in Hemiparetic Walking. Stroke. 2006;37:872–877. doi:10.1161/01.STR.0000204063.75779.8d.

12. Awad LN, Binder-Macleod SA, Pohlig RT, Reisman DS. Paretic propulsion and trailing limb angle are key determinants of long-distance walking function after

stroke. Neurorehabilitation and Neural Repair. 2015;29(6):499–508. 579
doi:10.1177/1545968314554625.Paretic. 580

13. Hsiao H, Knarr BA, Higginson JS, Binder-Macleod SA. Mechanisms to increase 581
propulsive force for individuals poststroke. Journal of Neuroengineering and 582
Rehabilitation. 2015;12(40). doi:10.1186/s12984-015-0030-8. 583

14. Peterson CL, Cheng J, Kautz SA, Neptune RR. Leg extension is an important 584
predictor of paretic leg propulsion in hemiparetic walking. Gait & Posture. 585
2010;32(4):451–456. doi:10.1016/j.gaitpost.2010.06.014. 586

15. Hsiao H, Knarr BA, Higginson JS, Binder-Macleod SA. The Relative 587
Contribution of Ankle Moment and Trailing Limb Angle to Propulsive Force 588
during Gait. Human Movement Science. 2015; p. 212–221. 589
doi:10.1016/j.humov.2014.11.008. 590

16. Ahn J, Hogan N. Walking is Not Like Reaching: Evidence from Periodic 591
Mechanical Perturbations. PLoS ONE. 2012;7(3). 592
doi:10.1371/journal.pone.0031767. 593

17. Zhang J, Fiers P, Witte KA, Jackson RW, Poggensee KL, Atkeson CG, et al. 594
Human-in-the-loop optimization of exoskeleton assistance walking. Science. 595
2017;356(June):1280–1284. doi:10.1126/science.aal5054. 596

18. Awad LN, Bae J, O'Donnell K, De Rossi SMM, Hendron K, Sloot LH, et al. A 597
soft robotic exosuit improves walking in patients after stroke. Science 598
Translational Medicine. 2017;9(400):eaai9084. doi:10.1126/scitranslmed.aai9084. 599

19. Turner DL, Ramos-Murguialday A, Birbaumer N, Hoffmann U, Luft A. 600
Neurophysiology of robot-mediated training and therapy: a perspective for future 601
use in clinical populations. Frontiers in Neurology. 2013;. 602

20. Kirtley C, Whittle MW, Jefferson RJ. Influence of walking speed on gait 603
parameters. Journal of Biomedical Engineering. 1985;7:282–288. 604
doi:10.1016/0141-5425(85)90055-X. 605

21. Riley PO, Croce UD, Kerrigan DC. Propulsive adaptation to changing gait speed. 606
Journal of Biomechanics. 2001;34:197–202. doi:10.1016/S0021-9290(00)00174-3. 607

22. Monaco V, Rinaldi LA, Macrì G, Micera S. During walking elders increase efforts at proximal joints and keep low kinetics at the ankle. Clinical Biomechanics. 2009;24(6):493–498. doi:10.1016/j.clinbiomech.2009.04.004.

23. Devita P, Copple T, Patterson J, Rider P, Long B, Steinweg K. Modulating step length during walking by young and old adults. In: ASB 2009;.

24. Allet L, IJzerman H, Meijer K, Willems P, Savelberg H. The influence of stride-length on plantar foot-pressures and joint moments. Gait and Posture. 2011;34:300–306. doi:10.1016/j.gaitpost.2011.05.013.

25. Latt MD, Menz HB, Fung VS, Lord SR. Walking speed, cadence and step length are selected to optimize the stability of head and pelvis accelerations. Exp Brain Res. 2007;184(2):201–209.

26. Hof AL. Scaling gait data to body size. Gait & Posture. 1996;4(3):222–223.

27. Kramer PA, Sarton-Miller I. The energetics of human walking: Is Froude number (Fr) useful for metabolic comparisons? Gait & Posture. 2008;27(2):209–215.

28. Alexander R. The gaits of bipedal and quadrupedal animals. The International Journal of Robotics Research. 1984;.

29. Hsiao H, Knarr BA, Higginson JS, Binder-Macleod SA. Mechanisms to increase propulsive force for individuals poststroke. Journal of NeuroEngineering and Rehabilitation. 2015; p. 12–40.

30. Pataky TC, Vanrenterghem J, Robinson MA. The probability of false positives in zero-dimensional analyses of one-dimensional kinematic, force and EMG trajectories. Journal of Biomechanics. 2016;49(9):1468–1476.

31. Pataky TC, Vanrenterghem J, Robinson MA. Zero-vs. one-dimensional, parametric vs. non-parametric, and confidence interval vs. hypothesis testing procedures in one-dimensional biomechanical trajectory analysis. Journal of Biomechanics. 2015;48(7):1277–1285.

32. Franklin DW, Wolpert DM. Computational mechanisms of sensorimotor control. Neuron. 2011;72(3):425–442. doi:10.1016/j.neuron.2011.10.006.
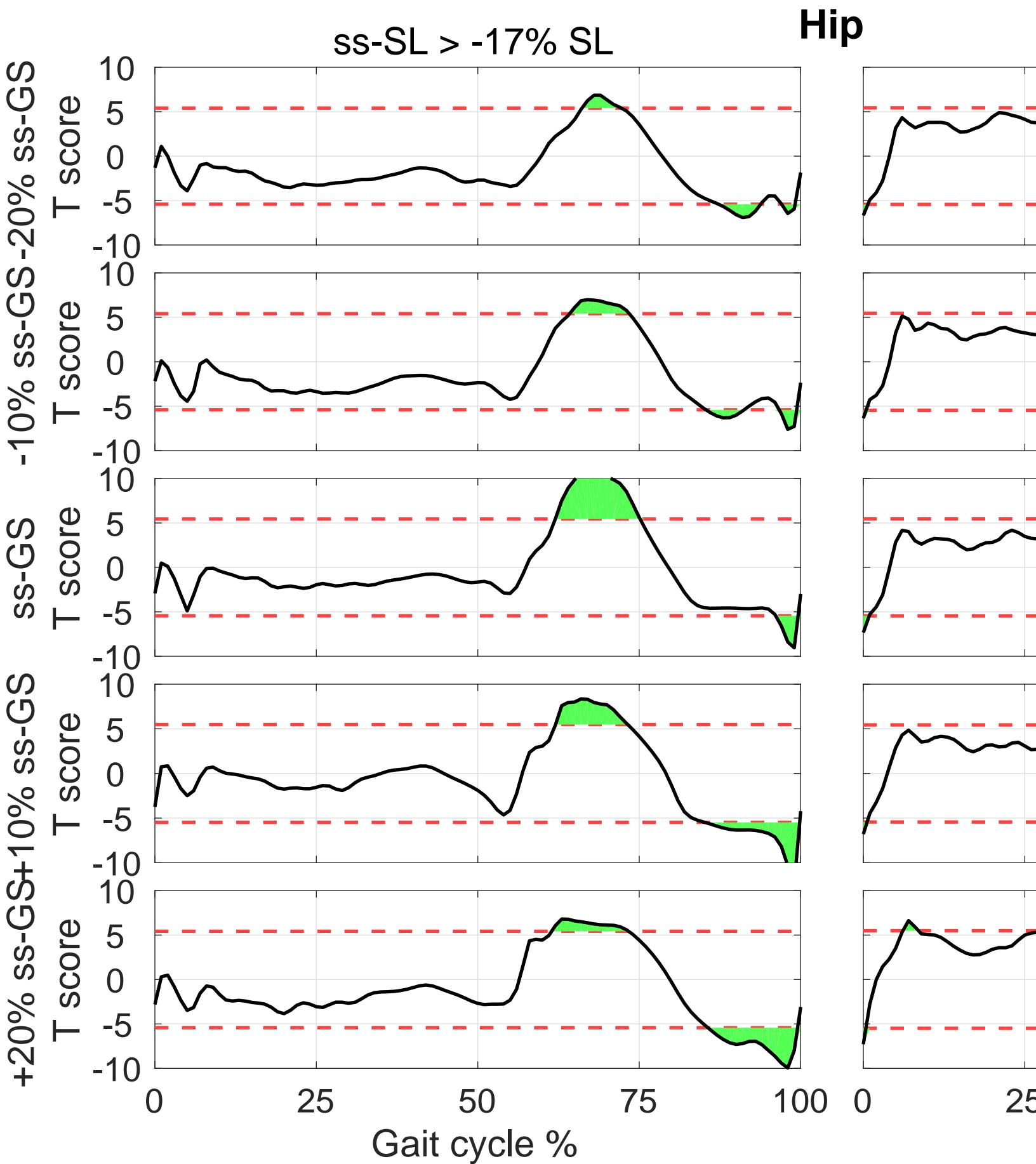
33. Prochazka A, Gillard D, Bennett DJ. Implications of positive feedback in the control of movement. Journal of Neurophysiology. 1997;77(6):3237–3251.
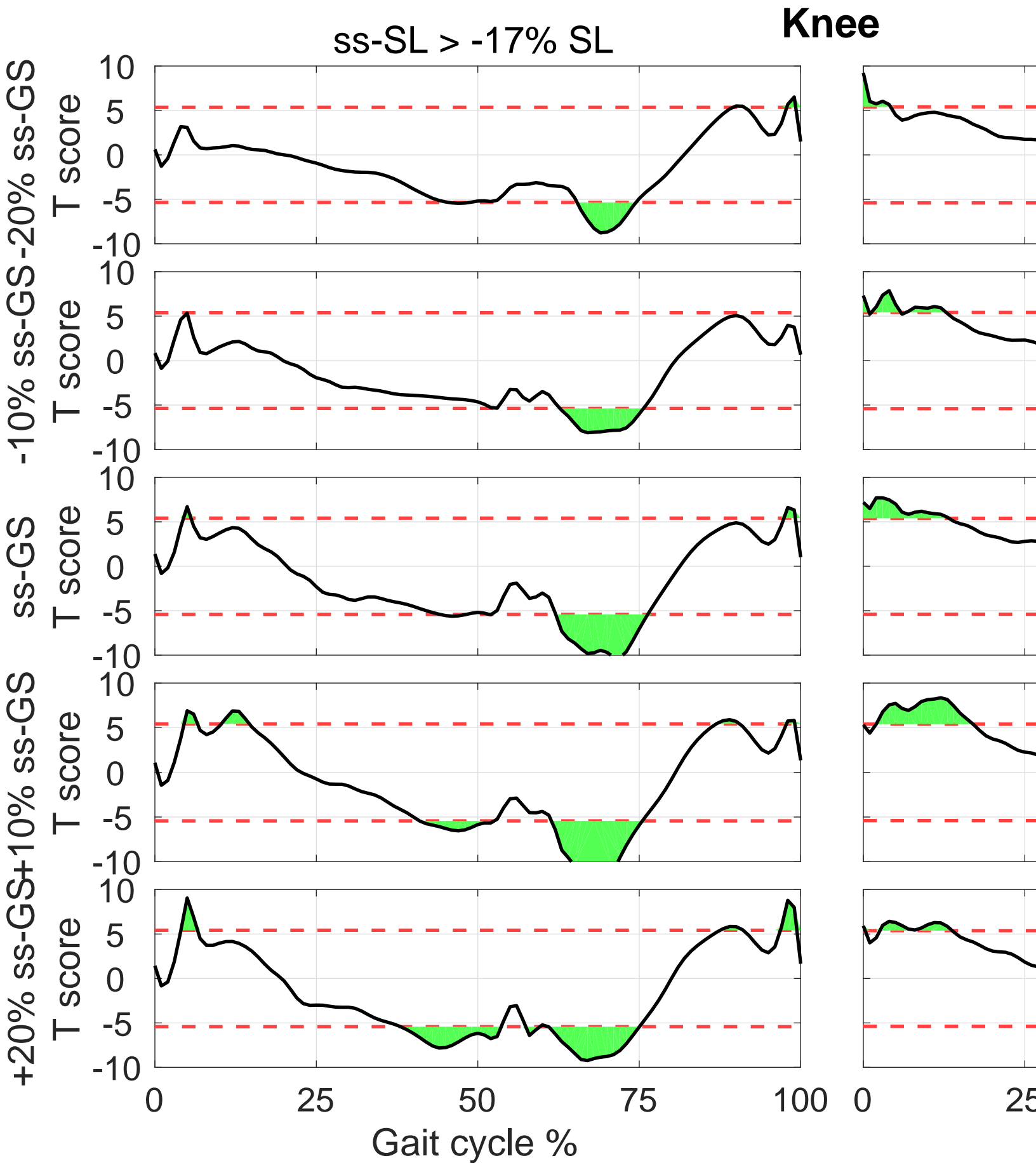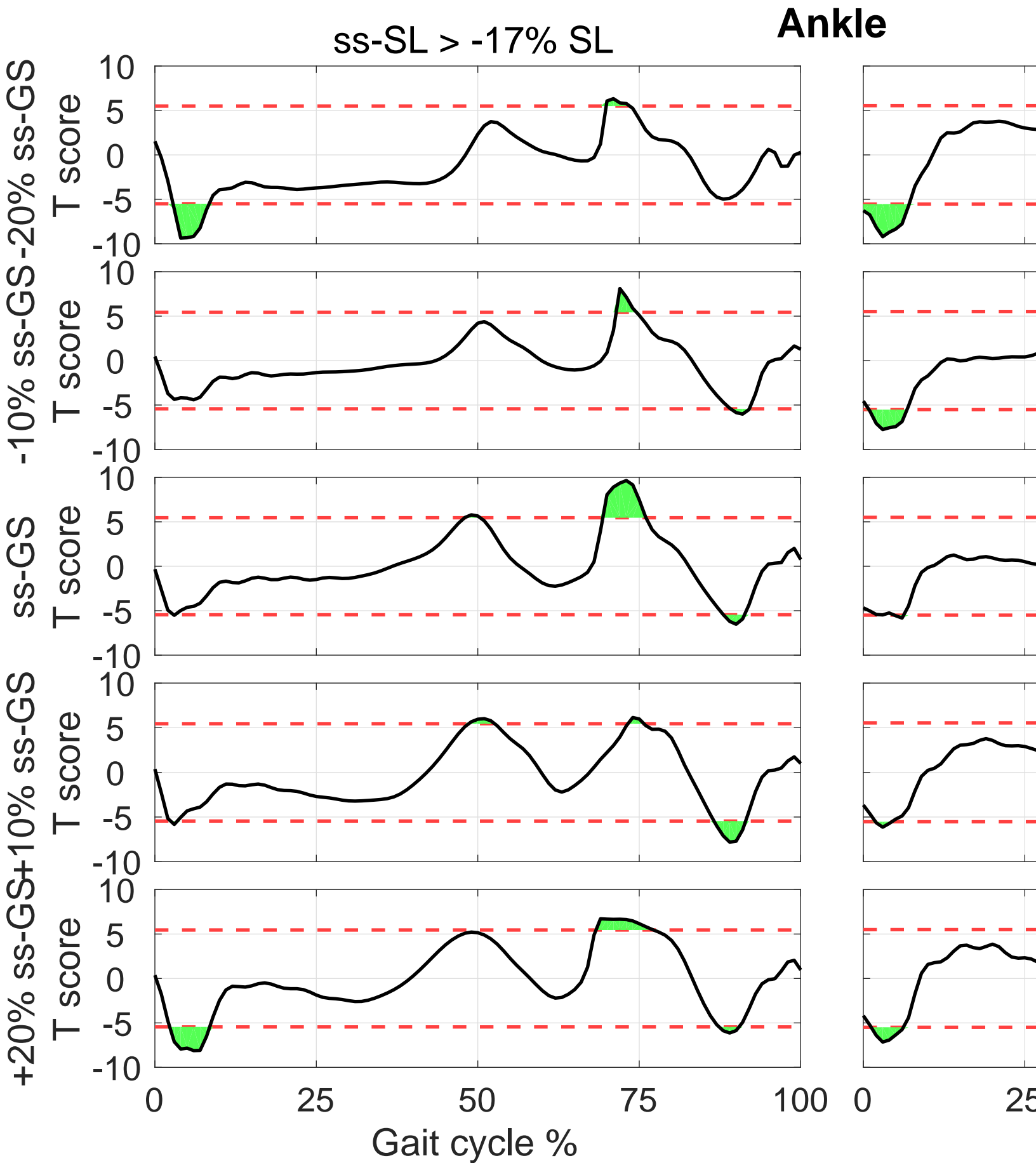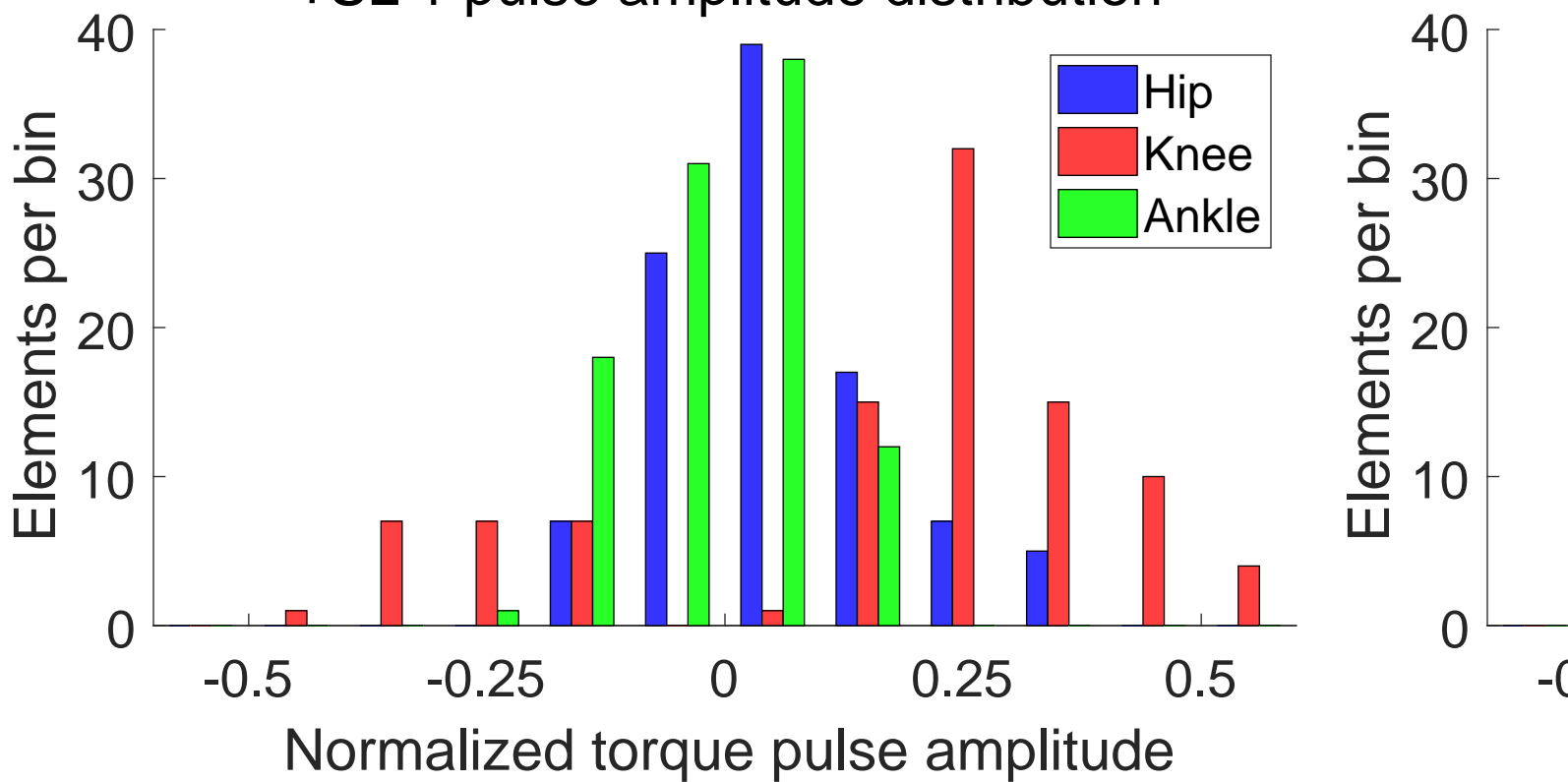
636

637
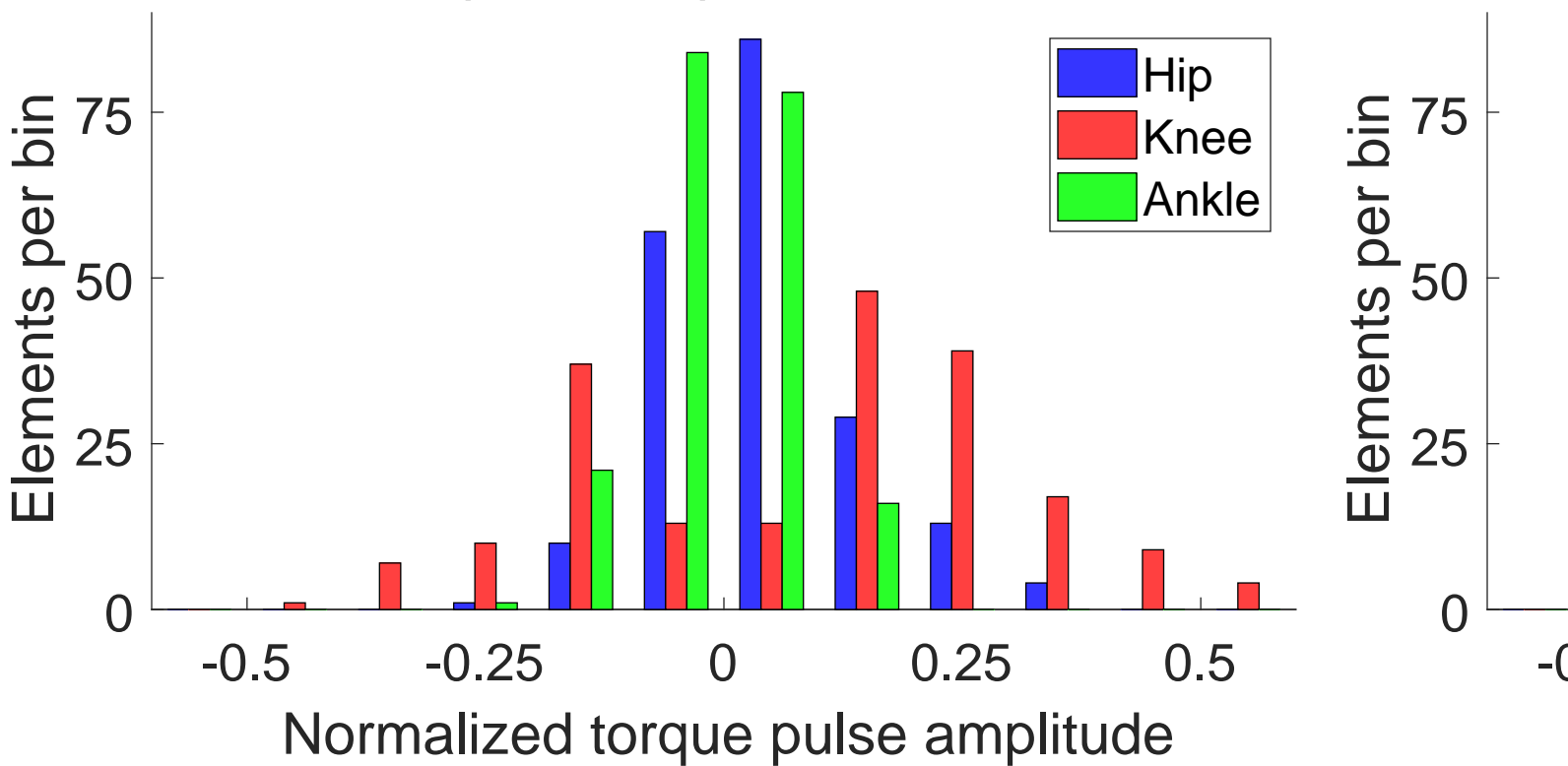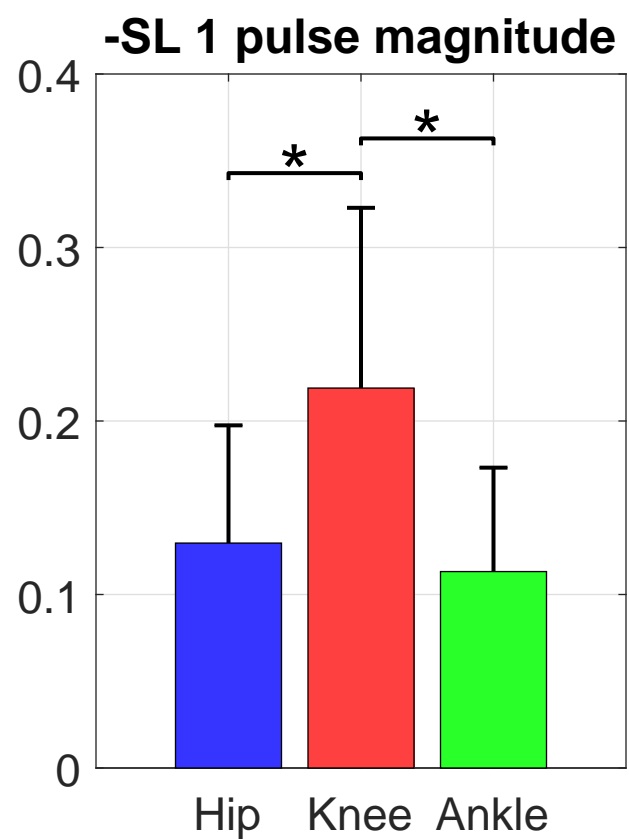
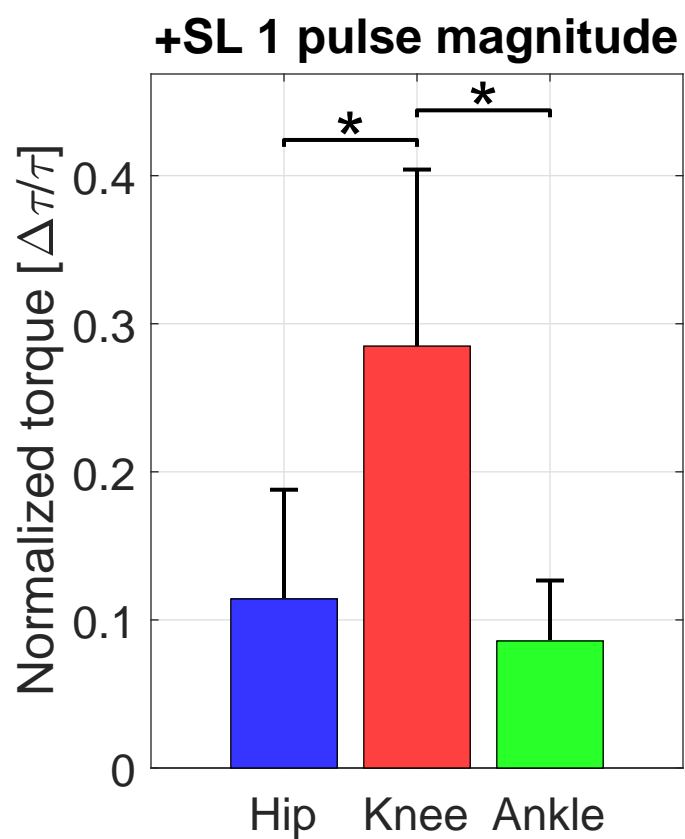**Hip**

Knee

ss-SL > -17% SL
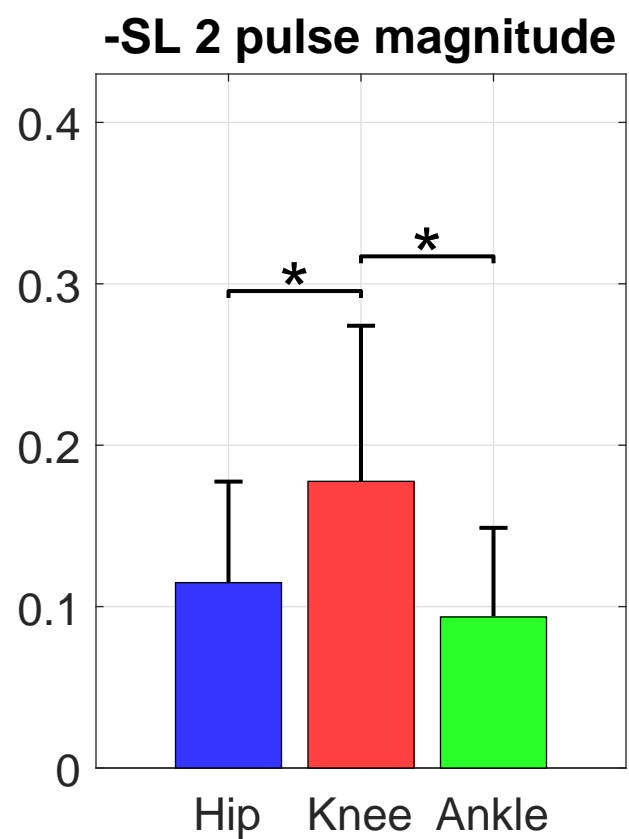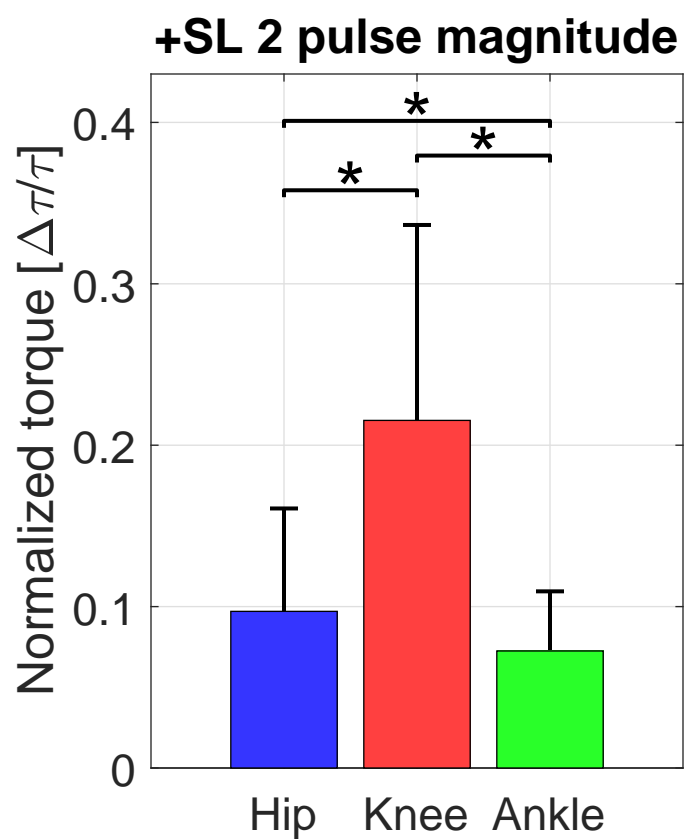
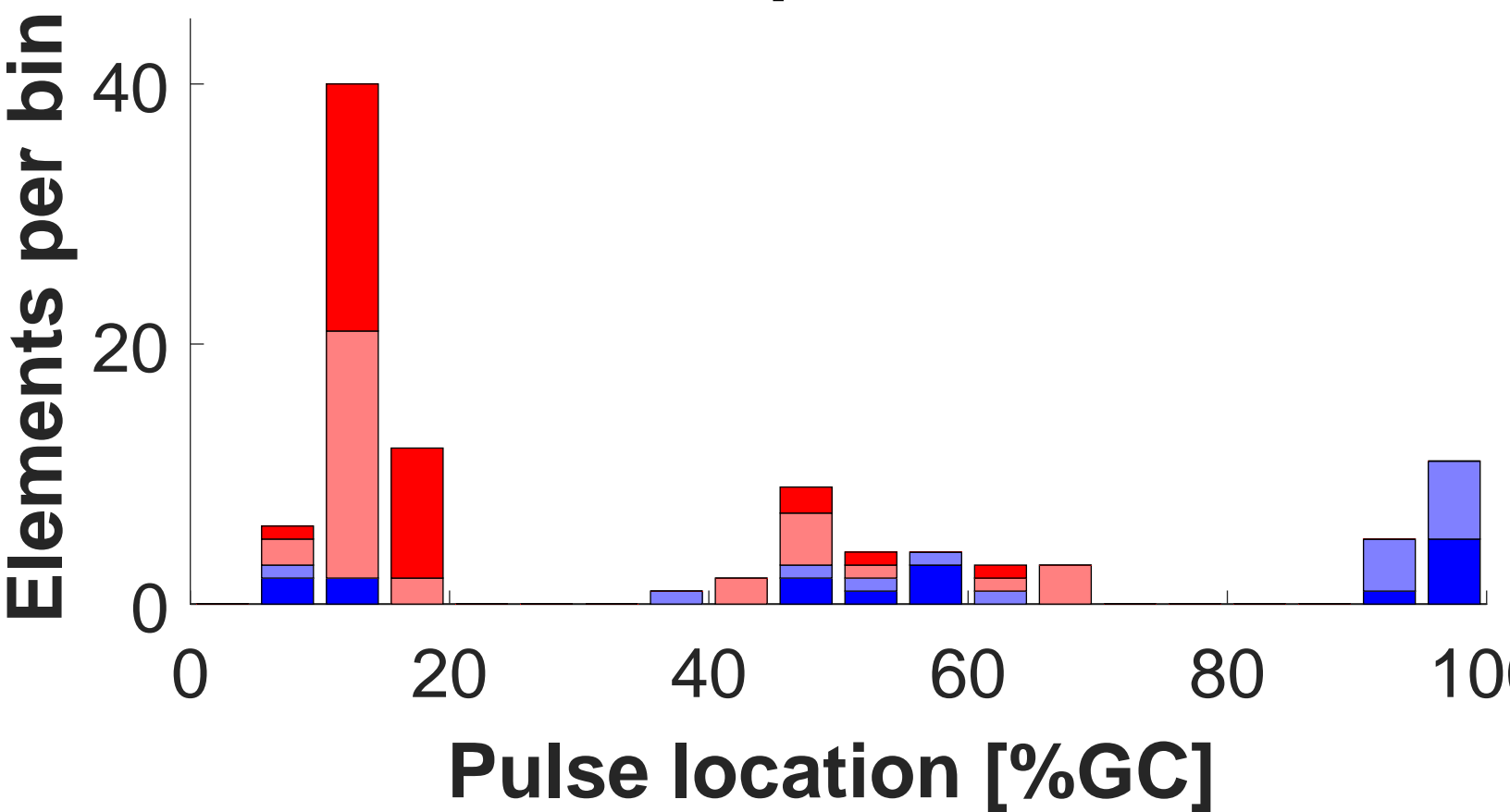**Ankle**

ss-SL > -17% SL
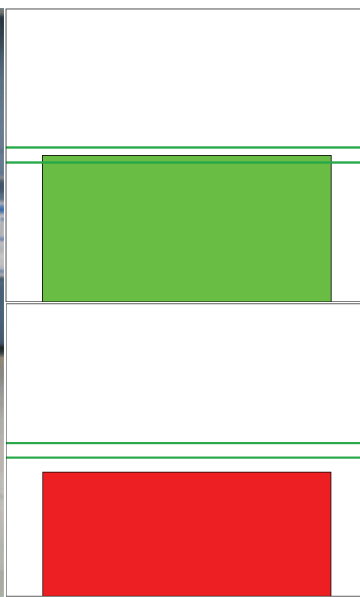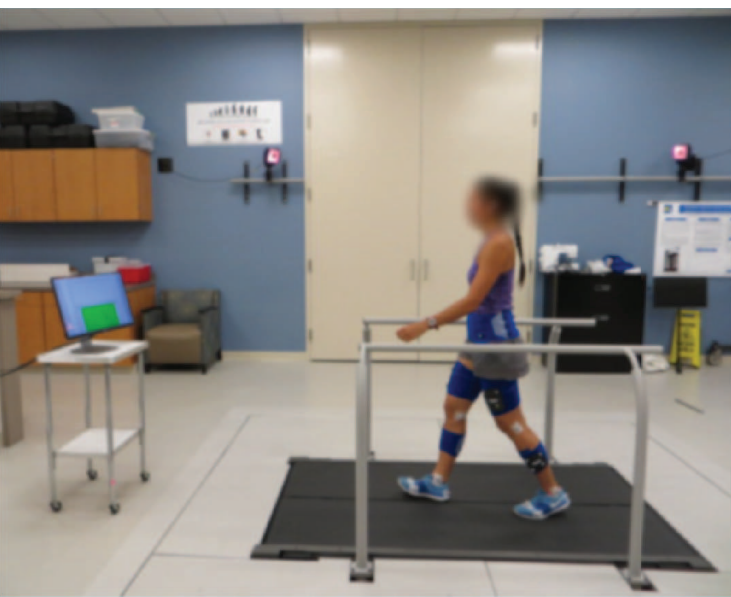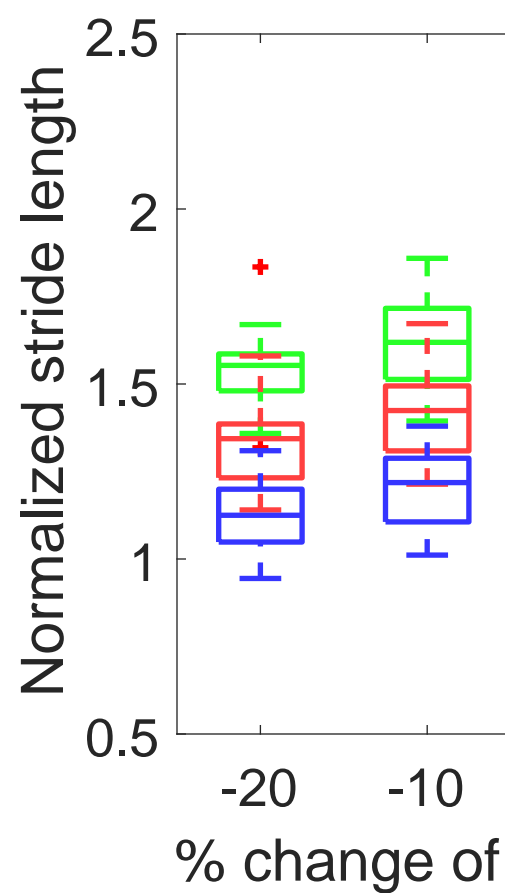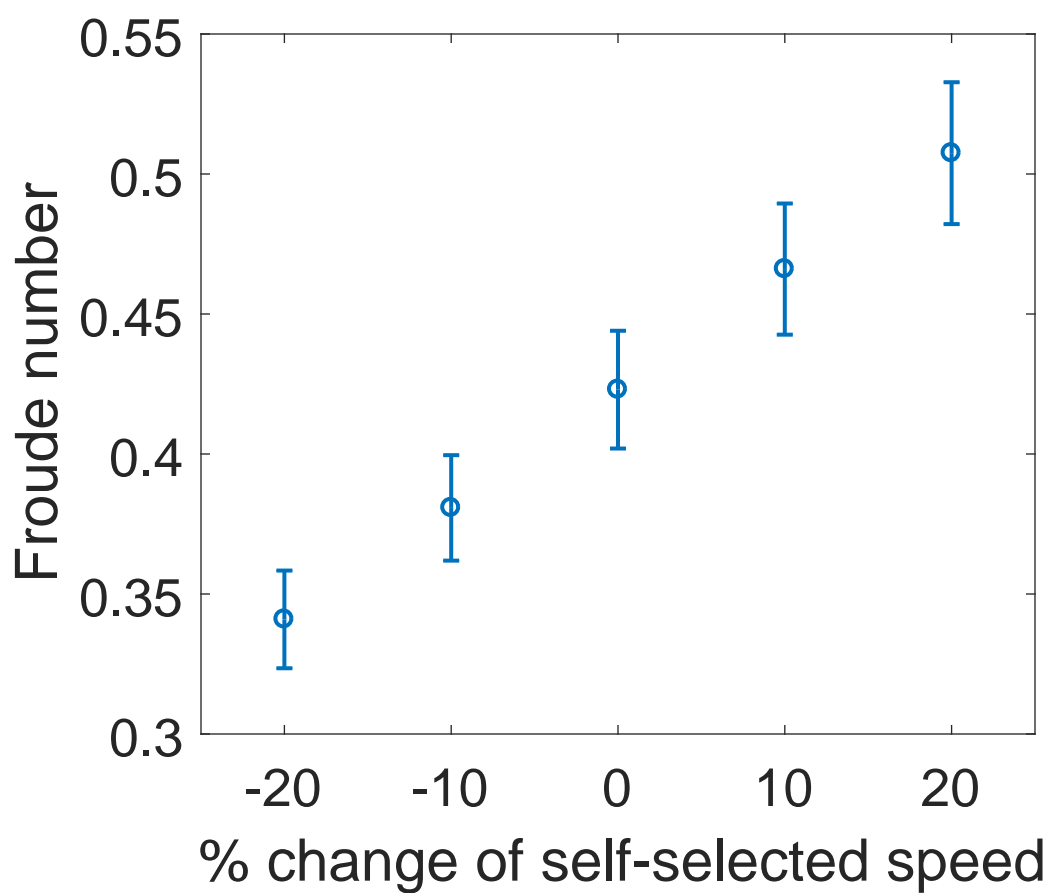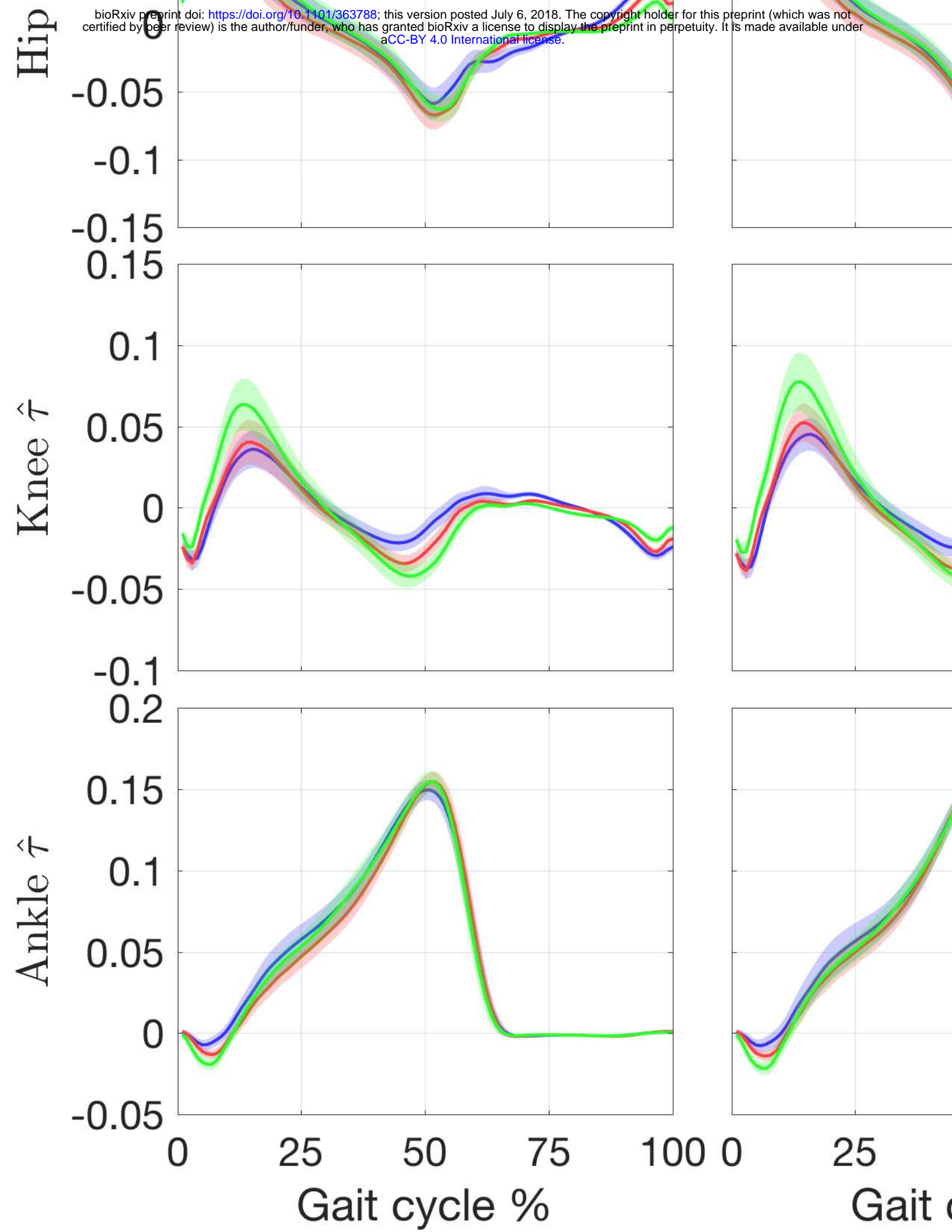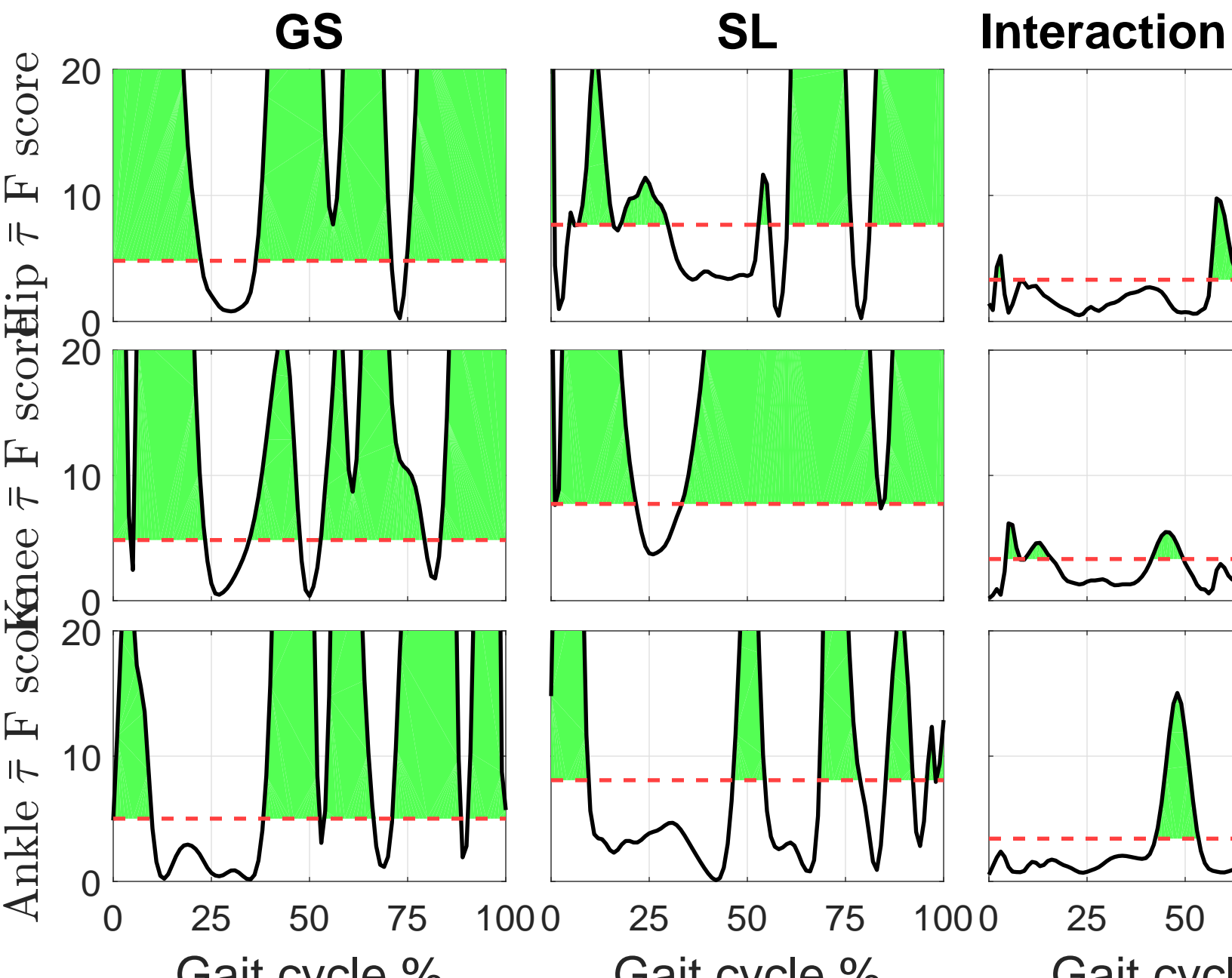
+SL 1 pulse amplitude distribution

+SL 2 pulse amplitude distribution

Hip +SL

Hip -SL